This article has been accepted for publication in a future issue of this journal, but has not been fully edited. Content may change prior to final publication. Citation information: DOI 10.1109/TWC.2018.2864734, IEEE Transactions on Wireless Communications

Self-Organizing Strategy Design for Heterogeneous Coexistence in the Sub-6 GHz

Marcello Caleffi, *Senior Member, IEEE*, Vito Trianni, Angela Sara Cacciapuoti, *Senior Member, IEEE*

***Abstract*—Due to the worldwide ongoing pressure to massively exploit the Sub-6 GHz spectrum for the deployment of independently-operated and heterogeneous networks, innovative solutions for the network coexistence are deeply required. Hence, in this paper, we design a self-organizing strategy with the aim of minimizing the coexistence interference among heterogeneous networks sharing the Sub-6 GHz spectrum. The design is performed under the constraints of promoting a selfless network utilization and avoiding any direct communication among the heterogeneous networks. For this, we develop an analytical framework, grounded on the nest-site selection behavior observed in honeybee swarms, to model the coexistence problem among multiple heterogeneous networks. Specifically, first, different heterogeneous networks are mapped into different *populations* and the allocation of a Sub-6 GHz band to a network is mapped into the population *commitment*. Then, the *evolution* of the commitment process is described through a multi-dimensional differential system. We analytically study the stability of such a system at the equilibrium, and we derive the conditions that assure the optimal allocation of the available Sub-6 GHz bands among the different heterogeneous networks. Finally, the proposed strategy is validated through an extensive performance evaluation.**

***Index Terms*—Sub-6 GHz, Heterogeneous Networks, Coexistence, Self-Organization, Collective Decision.**

I. Introduction

Despite the growing interest in higher spectrum bands such as millimeter wave (mmWave) and terahertz (THz) bands, it is worldwide recognized that the sub-6 GHz spectrum will play a crucial role for enabling mobile broadband communications within the next years [2], [3], [4], [5]. Recently, Huawei [6] reported that the Sub-6 GHz band will be "*the primary working frequency*" for the fifth generation (5G) of wireless networks. In June 2016, Qualcomm [7] announced a new 5G radio prototype working on the same band. In January 2017, Intel [8] unveiled a new 5G transceiver operating in both sub-6 GHz and mmWave bands, with initial support for the 3.3-4.2 GHz portion. Meanwhile, researchers and regulators [2], [9], [10] are actively working to find innovative solutions to efficiently use the sub-6 GHz spectrum, also by unlocking access to spectrum bands traditionally reserved to applications such as military, radar, and satellite. Examples include: i) worldwide, the 700 MHz band (694-790 MHz), the L-Band (1427-1518 MHz) and part of the C-Band (3.4-3.6 GHz), and ii) in some countries, further bands such as 470-694/698 MHz, 3.3-3.4 GHz, 3.6-3.7 GHz and 4.8-4.99 GHz.

In this dynamic scenario, it is very evident that the traditional *authorized/licensed* spectrum access model is ineffective [2], [11], and more efficient spectrum access models are required [3], [4] as the *opportunistic access model* [11], [12]. According to such a model, unlicensed users are allowed to opportunistically exploit temporal/spatial spectrum holes in a licensed band, given that the licensed communications are protected from harmful interference. The adoption of the opportunistic access paradigm is not limited to the 3.8-4.2 GHz band. Indeed, it represents the standard paradigm for the TV white space band (470-790 MHz) [13], [14], [15] and the 3.5 GHz band [16], and researchers are investigating its adoption also in radar bands [2].

According to the above argumentation, it is expected that, in the near future, multiple independently-operated and heterogeneous networks (HNs) will coexist within the same geographical area by opportunistically sharing one or multiple portions of the Sub-6 GHz spectrum. Indeed, the coexistence of these autonomous HNs requires innovative solutions for handling the coexistence interference. In fact, the heterogeneous interference is considerably much harder to handle than the same-technology interference [17], since the communication and coordination among HNs is precluded by the differences in terms of network architectures, hardware capabilities, wireless technologies, and protocol standards [18].

Hence, in this paper, we design a self-organizing coexistence strategy, with the aim of minimizing the coexistence interference among multiple HNs concurrently and opportunistically operating within the same Sub-6 GHz spectrum portion. The design is performed under two constraints: promoting a selfless network utilization of the spectrum and avoiding any direct communication among the HNs. For this, we model the coexistence problem among HNs as an optimal decentralized decision making problem, whereby a decision must be made to occupy the channel leading to the least coexistence interference. We introduce an analytical framework and a decentralized solution inspired by theoretical/experimental studies of the nest-site selection behavior of honeybees [19], [20]. Similarly to bees in a swarm searching and collectively deciding the best site where to build their hive, nodes in a HN search and collectively decide the best channel in which to communicate. Coexistence is achieved when multiple swarms/HNs minimally interfere with each other. To

A.S. Cacciapuoti and M. Caleffi are with DIETI, University of Naples Federico II, Naples, 80125 Italy (e-mail: angelasara.cacciapuoti@unina.it; marcello.caleffi@unina.it). They are also with the Laboratorio Nazionale di Comunicazioni Multimediali (CNIT), Naples, 80126 Italy.

V. Trianni is with ISTC, Consiglio Nazionale delle Ricerche, Rome, 00185 Italy (e-mail: vito.trianni@istc.cnr.it).

The preliminary version of this work has been presented at IEEE ICC 2016 [1]. This work was partially supported by the Italian National Program "Smart Cities and Communities" under grant "*S4E: Safety & Security Systems For Sea Environment*" and by the DIETI grant "*MARsHaL: Mobile Autonomous Robots for Hospital Logistics*".

This article has been accepted for publication in a future issue of this journal, but has not been fully edited. Content may change prior to final publication. Citation information: DOI 10.1109/TWC.2018.2864734, IEEE Transactions on Wireless Communications

this end, first, the different HNs are mapped into different *populations*, and the allocation of a channel to a HN is mapped into the *commitment* of the considered population. Then, the evolution of the population *commitment* is described with a multi-dimensional differential system. Through the paper, we analytically derive the equilibrium points of the differential system. Furthermore, we study the stability of the derived equilibria, and we derive the conditions for the strategy to guarantee an optimal spectrum allocation, i.e., the spectrum allocation minimizing the coexistence interference as detailed in Sec. IV-A. Finally, we conduct extensive numerical simulations by considering different performance criteria under different experimental conditions. The rest of the paper is organized as follows. In Sec. II, we introduce the network model along with some preliminaries. In Sec. III, we design the strategy. In Sec. IV, we analytically analyze the strategy optimality, whereas in Sec. V we carry out a discussion about the strategy implementation. In Sec. VI, we validate the theoretical analysis through a case study, and, finally, in Sec. VII, we conclude the paper.

A. Related Work and Contributions

Very recently, heterogeneous interference has been an important topic of research.

In [21], the authors proposed a cognitive coexistence scheme to enable spectrum sharing between unlicensed LTE networks and Wi-Fi networks, with the attractive feature of near-optimal spectrum access achieved with guaranteed fairness between unlicensed LTE and WiFi. In [22], the authors investigated the problem of LTE and WiFi coexisting in unlicensed spectrum. Specifically, they proposed three different coexistence mechanisms, and they showed that LTE can coexist with WiFi given that some LTE parameters are properly adapted. In [23], the authors studied the coexistence issues between IEEE 802.15.4g Smart Utility Networks and WiFi Networks, and they proposed a coexistence scheme based on cognitive radio technologies. In [24], the authors presented a network architecture to support the coexistence of WiFi and LTE cellular networks sharing the unlicensed spectrum. The proposal includes an interference avoidance scheme based on cellular networks estimating the density of nearby WiFi transmissions to facilitate the unlicensed spectrum sharing. Coexistence between WiFi and LTE in unlicensed bands has been studied also in [25], [26], [27], [28], [29], [30], [31]. The above works focused on the coexistence between two specific wireless technologies, and the proposed coexistence strategies strongly depend on the adopted layer-2 and -3 technologies. Moreover, they mostly require a certain form of communication and coordination between the different networks. In [17], the authors studied the coexistence problem from a different point of view, by proposing a strategy where coexisting networks cooperatively mitigate the interference to/from each other through interference cancellation to enhance everyone's performance. However, the proposal requires a strong cooperation among the coexisting networks and further studies on how to incentive such a cooperation are still required. In [32], the TV white space sharing among heterogeneous networks is modeled as a multi-objective optimization problem, and the authors designed an evolutionary centralized algorithm for the considered problem.

The most related papers to the work proposed in this manuscript are [33], [34]. In [33], the authors designed a coexistence strategy based on ecological species competition for TV White Space spectrum. However, in such a work the authors assumed the presence of a centralized coexistence manager and they required a certain degree of communication among the coexisting networks. In [34], the authors designed an optimal strategy for heterogeneous coexistence in TV White Spaces in absence of direct communications among the coexisting networks. However, the designed strategy is selfish, i.e., it maximized the expected throughput for the considered network by neglecting the impact of the strategy on the remaining networks. Differently from all the aforementioned works, we design a coexistence strategy:

- seamless, i.e., independent of (and not requiring any a-priori information about) the underlying wireless technologies;
- promoting a selfless network utilization of the spectrum;
- self-organizing, i.e., allowing each HN to reach a spectrum decision without the need of central entities or direct communications with the coexisting HNs.

These features are very demanding. In fact, so far, complete interoperability based on over-the-air communications among heterogeneous wireless technologies, regardless the involved technologies, is still missing [34]. The coexisting strategies available in literature are singled out accordingly to specific technologies, e.g., LTE/WiFi coexistence in the unlicensed band, and/or they resort to centralized entities to handle the coordination. Hence, an appealing characteristic of any heterogeneous coexistence strategy is to avoid direct communications among HNs, i.e., the capacity to face with dissimilar wireless technologies/standards. Moreover, selfish behaviors degrade the overall network performance [35], by allowing the detention of the communication resources only to specific HNs (e.g. the ones characterized by the best channel conditions or the highest transmitted power), so penalizing the remaining coexisting HNs. Hence, an appealing characteristic of any heterogeneous coexistence strategy is to be selfless to lead to a harmonious, efficient and fair utilization of the communication resources.

II. System Model and Preliminaries

We consider multiple independently-operated HNs operating within the Sub-6 GHz spectrum accordingly to the opportunistic spectrum access model. We denote with $\mathcal{N} = \{1, 2, \ldots, N\}$ and $\mathcal{C} = \{1, 2, \ldots, C\}$ the sets of coexisting HNs and available sub-6 GHz channels, respectively. Without loss of generality and in agreement with current regulations [13], [36], hereafter it is assumed that $\mathcal{C}$ is acquired through a geo-location database. The results derived in the following continue to hold if the set $\mathcal{C}$ is acquired differently, e.g. through traditional spectrum sensing techniques, since the proposed framework does not rely on the particulars of the adopted spectrum access technique.

This article has been accepted for publication in a future issue of this journal, but has not been fully edited. Content may change prior to final publication. Citation information: DOI 10.1109/TWC.2018.2864734, IEEE Transactions on Wireless Communications

TABLE I
ADOPTED NOTATION

Symbol	Definition
$\mathcal{N}$	set of coexisting secondary HNs
$\mathcal{C}$	set of available Sub-6 GHz channels
q_c^n	quality of the c-th channel for the n-th HN
$\mathcal{I}_c^n(t)$	the interference perceived by the n-th HN on channel c at time t
$\psi_c^n(t)$	fraction of nodes belonging to the n-th HN committed to channel c at time t
$\psi_u^n(t)$	fraction of nodes belonging to the n-th HN uncommitted at time t
$\gamma_c^n(t)$	(spontaneous) c-th channel commitment rate for the uncommitted fraction of the n-th population at time t
$\alpha_c^n(t)$	(spontaneous) abandon rate for the fraction of the n-th population committed to channel c at time t
$\rho_c^n(t)$	c-th channel recruitment rate for the fraction of the n-th uncommitted population at time t
$\sigma_\ell^n(t)$	inhibition rate induced by the fraction of the n-th population committed to channel ℓ the at time t

Each HN in $\mathcal{N}$ selects one of the channels in $\mathcal{C}$ through the concept of *commitment*. Specifically, the n-th HN is modeled as a population of agents or nodes. We assume that an agent coincides with a node, and we will use the two terms as synonymous in the following. This assumption is not restrictive: the results derived in the following continue to hold either if: i) multiple agent instances are executed within a single node, or ii) a single agent characterizes several nodes, as long as the agent communication demand is consistently scaled. Each node contributes to the channel selection process through its *commitment* state. Accordingly, a node in favor of using the c-th channel is said to be *committed* to such a channel, otherwise, it is said to be *uncommitted*. Once the entire population (or a sufficient fraction as detailed in Sec. V-B) representing the n-th HN is committed to the same channel, then such a channel is selected by the HN for its communication needs. In the following, we denote with $\psi_c^n(t)$ the fraction of the n-th population committed to channel c at the time t, and with $\psi_u^n(t)$ the corresponding uncommitted fraction.

The commitment process, i.e., the preference of the arbitrary n-th network toward the c-th channel, depends on several factors, such as the network throughput demand and the channel data rate, which in turns depends on the particulars of the wireless communication system adopted by each HN as well as the signal-to-noise ratio experienced on such a channel plus the interference experienced on the same channel. As instance, channels with different data rates can be equally preferable as long as they both accommodate the network demand. In the following, we gather some definitions used, while Table I summarizes the notation adopted within the manuscript.

Definition 1. (Channel Quality) We model the quality of channel c perceived by the n-th network in absence of coexistence interference through the dimensionless non-negative quantity $q_c^n \in [0,1]$, referred to as *channel quality*. Hence, $q_c^n = 0$ represents the *adverse* channel whereas $q_c^n = 1$ denotes the *ideal* channel for the n-th network.

Definition 2. (Coexistence Interference) The dimensionless non-negative quantity $\mathcal{I}_c^n(t)$ represents the coexistence interference perceived by the n-th HN on channel c at time t. Hence, $\mathcal{I}_c^n(t) = 0$ denotes the *absence* of interference, whereas $\mathcal{I}_c^n(t) = 1$ denotes channel c being *saturated* by the transmissions of the coexisting HNs.

Through the general concepts of quality and interference, we abstract from the particulars (modulation, power control, propagation, etc.) of the wireless technology adopted by each HN, focusing so our attention on the coexistence strategy design and performance. The abstraction from the particulars is very common in literature [32], [34], since it leads to tractable mathematical analyses without any loss of generality. In fact, by substituting in q_c^n and $\mathcal{I}_c^n(t)$ physical-layer compliant expressions, the analysis conducted within the manuscript continues to hold, since it does not rely on these specific expressions.

Both the channel quality and the coexistence interference need to be calculated to practically implement the proposed coexistence strategy. Hence, in Sec. V we present a possible choice to calculate both quantities. As an example, the channel quality is obtained by opportunely normalizing the Shannon capacity achievable by the n-th network on channel c. Nevertheless, as said, the conducted analysis does not rely on the specific choice made for the estimation/calculation procedure, due to the abstraction from the particulars allowed by the general concepts of quality and interference. Hence, any alternative for estimating the aforementioned quantities can be adopted without affecting the generality of the analysis.

III. STRATEGY DESIGN

In this Section we design the proposed coexisting strategy. Specifically, we first map the different HNs into different populations, and the allocation of a channel to a HN into the commitment of the considered population. Then the commitment dynamics among different populations are carefully designed to effectively account for the trade-off between selfish behavior and fair sub-6 GHz spectrum allocation. To this aim, the evolution of the population commitment is modeled through a multi-dimensional differential system, according to which each population commitment is driven by four different processes as described in Sec. III-A. According to this evolution, each HN distributively, autonomously and adaptively selects to use one of the available channels once its entire population (or a sufficient fraction) is committed to the same channel.

A. Population Dynamics

To design the coexisting strategy, we exploit a recently proposed framework for collective decision-making in presence of a single population [19], [20], by generalizing it to a multi-dimensional framework through the introduction of multiple concurrent populations and by accounting for the peculiar communication issues characterizing a coexisting network scenario in the Sub-6 GHz spectrum. The framework is grounded on experimental/theoretical studies of the nest-site selection behavior observed in honeybee swarms (*Apis mellifera*) [37], [38], [39].

This article has been accepted for publication in a future issue of this journal, but has not been fully edited. Content may change prior to final publication. Citation information: DOI 10.1109/TWC.2018.2864734, IEEE Transactions on Wireless Communications

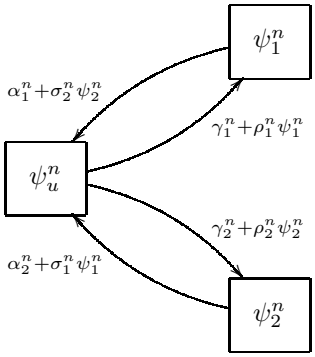

Fig. 1. The n-th population (HN) dynamics for two channels. ψ_u^n represents the fraction of uncommitted agents, whereas ψ_1^n and ψ_2^n represents the fraction of agents committed to channel 1 and 2. Time dependence omitted for the sake of simplicity.

Specifically, let us consider N different HNs and C available channels in a certain network coexisting area. As shown in Fig. 1, the commitment dynamic (i.e., channel preference) of each population (i.e., each HN) is proposed to evolve according to four concurrent processes:

i) *abandonment*: the nodes of the n-th HN committed to channel $c \in \mathcal{C}$ spontaneously *abandon* the commitment (i.e., become uncommitted) at rate $\alpha_c^n(t)$;
ii) *commitment*: the uncommitted nodes of the n-th HN spontaneously *commit* to channel $c \in \mathcal{C}$ at rate $\gamma_c^n(t)$;
iii) *inhibition*: the nodes of the n-th HN committed to channel $c \in \mathcal{C}$ are *inhibited* (i.e., become uncommitted) by nodes of the same HN committed to channel $\ell \in \mathcal{C}$, $\ell \neq c$, at rate $\sigma_\ell^n(t)$;
iv) *recruitment*: the nodes of the n-th HN committed to channel $c \in \mathcal{C}$ *recruit* uncommitted nodes belonging to the same HN at rate $\rho_c^n(t)$.

Stemming from the above processes, we propose to model the overall dynamics of the N different HNs through the system of $C \times N$ coupled differential equations in (1), with the N population conservation equations given in (2) forcing the commitment dynamics within feasible bounds, i.e., imposing the sum of the fraction of nodes $\psi_c^n(t), \psi_u^n(t)$ being equal to one for each population:

$$\begin{aligned}\dot{\psi_c^n}(t) =&\gamma_c^n(t)\psi_u^n(t) - \alpha_c^n(t)\psi_c^n(t) + \rho_c^n(t)\psi_c^n(t)\psi_u^n(t)+ \\ &- \psi_c^n(t)\sum_{\ell\neq c}\sigma_\ell^n(t)\psi_\ell^n(t),\ \forall c \in \mathcal{C}, n \in \mathcal{N} \qquad (1)\end{aligned}$$

$$\psi_u^n(t) = 1 - \sum_{c\in\mathcal{C}}\psi_c^n(t), \quad n \in \mathcal{N} \qquad (2)$$

Two different types of dynamics can be recognized: a) *spontaneous* dynamics independent of the population commitment state, driven by $\gamma_c^n(t)$ and $\alpha_c^n(t)$; b) *interactive* dynamics depending on the population commitment states, driven by $\rho_c^n(t)$ and $\sigma_c^n(t)$.

B. Transition Rates Setting

From Sec. III-A, it results that the setting of the transition rates drives the HN commitment dynamics and hence the performance of the coexisting strategy. In this paper, we aim at promoting a selfless utilization of the Sub-6 GHz spectrum among multiple co-located HNs. Nevertheless, such a selfless utilization must also be effective, i.e., it must avoid naive selfless allocations in which some of the HNs decide not to utilize any of the available channels. Stemming from all these considerations, we adopt the following transition rate setting and we show in Sec. IV the analytical performance of such a setting:

$$\begin{aligned}&\gamma_c^n(t) \propto q_c^n, \qquad &&\alpha_c^n(t) \propto \frac{1-\psi_c^n(t)}{q_c^n}\,\mathcal{I}_c^n(t) \\ &\rho_c^n(t) \propto q_c^n, \qquad &&\sigma_{\ell,\ell\neq c}^n(t) \propto q_\ell^n\end{aligned} \qquad (3)$$

where q_c^n and $\mathcal{I}_c^n(t)$ are introduced in Defs. 1 and 2. First of all, we note that all transition rates depend on the channel quality q_c^n. This allows to properly define the *intra-population dynamics* leading to the choice of a unique channel c for the n-th HN, and providing the *selfish pressure* for using the most favorable channel. More precisely, the commitment to channel c—modeled by $\gamma_c^n(t)$ and $\rho_c^n(t)$—increases linearly with q_c^n. This choice is reasonable and valuable. In fact, the more a channel is appealing, the more likely an agent should commit to it, either spontaneously or by being recruited. The abandonment rate $\alpha_c^n(t)$, instead, is inversely proportional to q_c^n. Again, this choice is reasonable, since the more a channel is appealing, the less likely an agent should abandon it. Finally, the negative feedback modeled by $\sigma_{\ell,\ell\neq c}^n(t)$ increases linearly with q_ℓ^n. The rationale is the following: the more channel ℓ is appealing, the more likely an agent committed to a different channel should be inhibited. All the transition rates are constant except the abandonment rate $\alpha_c^n(t)$, which is exploited to capture the *inter-population dynamics*. Indeed, $\alpha_c^n(t)$ adaptively drives the system toward a fair interference-aware channel selection by accounting for the presence of different HNs communicating on the same channel through the factor $\mathcal{I}_c^n(t)$. The rationale for this choice is the following: the higher is the expected interference level affecting a given channel, the more likely an agent should abandon the channel. Hence, $\alpha_c^n(t)$ represents the *selfless behavior* forcing each population toward a fair spectrum allocation. Furthermore, $\alpha_c^n(t)$ increases linearly with $1-\psi_c^n(t)$. The choice is rationale: the more a population occupies a channel, the less it would be prone to abandon it, leading to a null abandonment when the population is completely allocated to the same channel.

In a nutshell, the commitment rate $\gamma_c^n(t)$ allows a population to select the channel with higher quality. The recruitment rate $\rho_c^n(t)$ and the inhibition rate $\sigma_c^n(t)$ drive the agents within the same population to commit to the same channel, i.e., they represent the *consensus pressure*. The abandonment rate $\alpha_c^n(t)$ adaptively drives the system toward a fair interference-aware channel selection by accounting for the presence of different HNs communicating on the same channel. In Sec. V, we discuss on the realistic strategy implementation by giving insights on how to calculate the required quantities.

IV. Theoretical Analysis

Here, we analytically assess the performance of the proposed strategy through the stability theory, by first deriving

This article has been accepted for publication in a future issue of this journal, but has not been fully edited. Content may change prior to final publication. Citation information: DOI 10.1109/TWC.2018.2864734, IEEE Transactions on Wireless Communications

the equilibrium points of the strategy and then by assessing their stability.

A. Preliminaries

Definition 3. (Equilibrium Point) Given the $C \times N$ differential equations in (1) under constraint (2) with transition rates as in (3), an equilibrium point $\mathbf{x} = (x_1^1, \ldots, x_C^1, x_1^2, \ldots, x_C^N) \in [0,1]^{C\,N}$ is a constant solution of (1), i.e., $\dot{\psi}_c^n(t) = 0$ when $\psi_c^n(t) = x_c^n$ for any $t > 0$, $c \in \mathcal{C}$ and $n \in \mathcal{N}$:

$$\dot{\psi}_c^n(t)|_{\psi_c^n(t)=x_c^n} = 0, \ \forall\, n, c \tag{4}$$

To have a tractable analytical problem and to abstract from the particulars of the wireless propagation, we consider the interference being proportional to the sum of the fraction of nodes of different HNs committed to the same channel, i.e.:

$$\mathcal{I}_c^n(t) \approx \sum_{m \neq n} \psi_c^m(t) \tag{5}$$

and, in the following, we denote with $\mathcal{I}_c^n(\mathbf{x})$ the coexistence interference perceived by the n-th HN on the c-th channel at the equilibrium point $\mathbf{x}$, i.e., $\mathcal{I}_c^n(\mathbf{x}) \approx \sum_{m \neq n} x_c^m$.

Remark. The rationale for this choice is the following: the more are the nodes of the different HNs committed to a given channel, the higher is the expected interference level affecting such a channel. Although the aforementioned choice is reasonable, in Sec. VI, we validate the proposal against the theoretical analysis conducted here, by comparing the strategy approximating the interference as in (5) with the strategy accounting for the effective level of interference.

Definition 4. (Consensus Indicator) Let us denote with $1_c^n(\mathbf{x})$ the binary variable indicating whether the n-th HN is fully committed to the c-th channel at the equilibrium $\mathbf{x}$, i.e. $1_c^n(\mathbf{x}) = 1$ if $x_c^n = 1$ and $1_c^n(\mathbf{x}) = 0$ otherwise (indeed, from (2), we have that if it exists $\tilde{c} \in \mathcal{C} : x_{\tilde{c}}^n = 1$, then $x_c^n = 0 \ \forall\, c \neq \tilde{c}$.). In the following, $\mathbf{1}(\mathbf{x})$ denotes the $\mathcal{N} \times \mathcal{C}$ matrix collecting the consensus indicators for each HN and for each channel at the equilibrium $\mathbf{x}$.

Definition 5. (Spectrum Allocation) An equilibrium point $\mathbf{x}$ denotes a *valid spectrum allocation solution* of the proposed strategy if each HN reaches full consensus, i.e., if for any $n \in \mathcal{N}$ it exists an arbitrary $\tilde{c} \in \mathcal{C} : 1_{\tilde{c}}^n(\mathbf{x}) = 1$.

Remark. In Def. 5, the full consensus constraint is required to assure that all the nodes of a HN communicate on the same channel, once the strategy converges toward a solution. Indeed, a pair of nodes of a HN, which want to communicate with each other, should rendezvous on a common channel before carrying on data transmissions.

Definition 6. (Optimal Spectrum Allocation) Any valid spectrum allocation is referred to as the optimal spectrum allocation $\tilde{\mathbf{x}}$ if it maximizes the overall channel quality by accounting for the channel interference, i.e., it maximizes the following metric:

$$\mathcal{Q}(\mathbf{x}) = \sum_{c \in \mathcal{C}} \left(\sum_{n \in \mathcal{N}} (1 - I_c^n(\mathbf{x})) q_c^n 1_c^n(\mathbf{x}) \right) \tag{6}$$

In the following we consider three different scenarios: 1) a single network and two Sub-6 GHz channels; 2) two HNs and two Sub-6 GHz channels; 3) N HNs and C available Sub-6 GHz channels. Scenarios 1 and 2 seldom happen in real applications. Nevertheless, we consider them before the general case represented by Scenario 3 since the mathematical analysis is very challenging and not previously conducted. Hence, analyzing first Scenarios 1 and 2 allows us to generalize easier the analysis of Scenario 3, i.e., for an arbitrary number of networks.

B. Scenario 1: Single Network

Here, we consider a single network and two available Sub-6 GHz channels. We assume, without lack of generality, $q_1^1 \leq q_2^1$, i.e., the first channel being not preferable with respect to the second one. According to Def. 6, the optimal spectrum allocation is the one assuring that the network is fully committed to the second channel, i.e., $\tilde{\mathbf{x}} = (0,1)$. By defining $k \triangleq q_1^1/q_2^1$, the following results hold.

Lemma 1. ***(Equilibria)*** *The set E of the equilibrium points of the proposed strategy is:*

$$E = \begin{cases} \{\mathbf{x}_0; \mathbf{x}_1\} & \text{if } 0 < k \leq \frac{1}{\sqrt{2}} \\ \{\mathbf{x}_0; \mathbf{x}_1; \mathbf{x}_2(k)\} & \text{if } \frac{1}{\sqrt{2}} < k \leq 1 \end{cases} \tag{7}$$

with $\mathbf{x}_0 = (0,1)$, $\mathbf{x}_1 = (1,0)$, and $\mathbf{x}_2(k) = \left(x_1^1(k), x_2^1(k)\right)$ shown in Fig. 2 and given by:

$$x_1^1(k) = \frac{1}{2}\left(\frac{1}{k} + \frac{2}{1+k+k^2} + \sqrt{\frac{1}{k^2} + \frac{4}{(1+k+k^2)^2}} - 2\right)$$
$$x_2^1(k) = \frac{-k + k x_1^1(k)^2}{-k - x_1^1(k) - k x_1^1(k)} \tag{8}$$

Proof: See Appendix A ■

Remark. The set E is composed by two disjointed equilibrium regions depending on the value of k, with threshold equal to $1/\sqrt{2}$. This is a valuable result: the equilibria do not depend on the individual values of q_1^1 and q_2^1 but rather on the ratio between the two values. In other words, one single parameter, namely, k, drives the system evolution, as proved in Proposition 1. Furthermore, the equilibrium point $\mathbf{x}_0$ is the optimal spectrum allocation $\tilde{\mathbf{x}}$ since: i) there exists a consensus, i.e., all the agents are committed to the same channel; ii) the consensus is reached toward the most preferable channel, i.e., the second channel. Differently, $\mathbf{x}_1$ represents a suboptimal allocation, since there exists a consensus but not toward the preferred channel unless $k = 1$, when both $\mathbf{x}_0$ and $\mathbf{x}_1$ represent the optimal spectrum allocation being the channel qualities equivalent. Finally, $\mathbf{x}_2$ does not allow to reach a full consensus, as show in Fig. 2. Hence, $\mathbf{x}_2$ is not a valid allocation.

Proposition 1. ***(Stability)*** *$\mathbf{x}_0$ is an asymptotically stable equilibrium point for any $k \in (0,1]$. Differently, $\mathbf{x}_1$ is an asymptotically stable equilibrium point for any $k \in (1/\sqrt{2}, 1]$, and an unstable equilibrium point for any $k \in (0, 1/\sqrt{2}]$. Finally, $\mathbf{x}_2$ is an unstable equilibrium point for any $k \in (1/\sqrt{2}, 1]$.*

Proof: See Appendix B ■

This article has been accepted for publication in a future issue of this journal, but has not been fully edited. Content may change prior to final publication. Citation information: DOI 10.1109/TWC.2018.2864734, IEEE Transactions on Wireless Communications

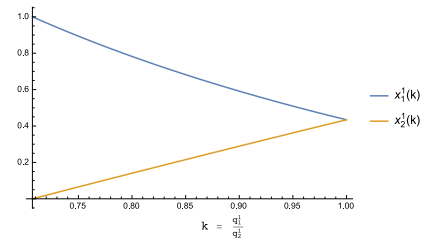

Fig. 2. Scenario 1: values of the components of the equilibrium point $\mathbf{x}_2(k) = (x_1^1(k), x_2^1(k))$ as a function of k.

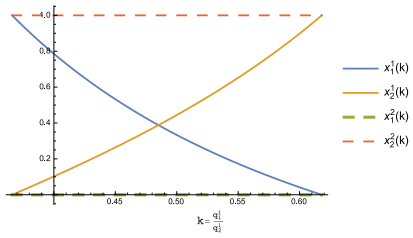

Fig. 3. Scenario 2: values of the components of the equilibrium point $\mathbf{x}_4(k) = (x_1^1(k), x_2^1(k), x_1^2(k), x_2^2(k))$ as a function of k.

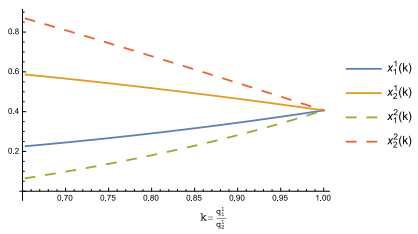

Fig. 4. Scenario 2: values of the components of the equilibrium point $\mathbf{x}_5(k) = (x_1^1(k), x_2^1(k), x_1^2(k), x_2^2(k))$ as a function of k.

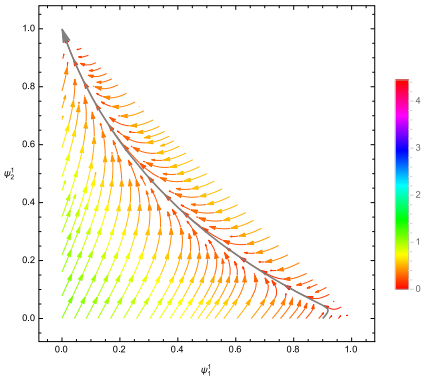

Fig. 5. Scenario 1: phase portrait for $k = 1/2$ colored according to the vector field norm. Gray trajectory starting from initial conditions $(0.9, 0)$.

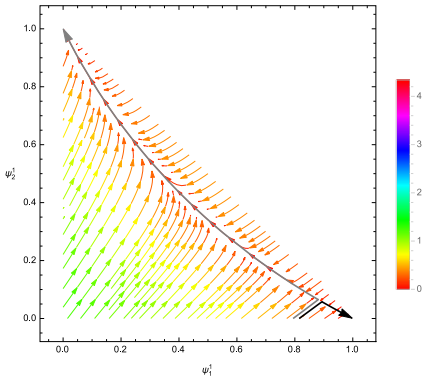

Fig. 6. Scenario 1: phase portrait for $k = 3/4$. Gray and black trajectories starting from initial conditions in the ϵ-neighborhood of $(0.8, 0)$.

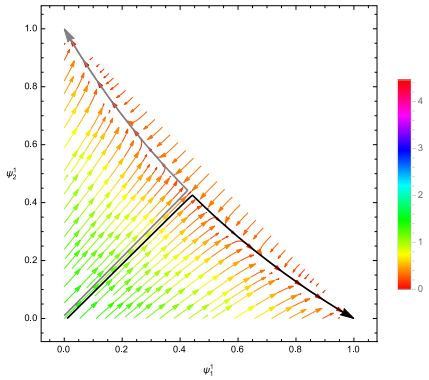

Fig. 7. Scenario 1: phase portrait for $k = 1$. Gray and black trajectories starting from initial conditions $(0.01, 0)$ and $(0, 0.01)$ respectively.

Stemming from Proposition 1, we have two cases.

1) $k \in (0, 1/\sqrt{2}] \iff 0 < q_1^1 \leq q_2^1/\sqrt{2}$: The system always evolves toward $\mathbf{x}_0$, i.e., toward the optimal spectrum allocation $\tilde{\mathbf{x}}$, regardless of the initial conditions $\psi_1^1(0)$ and $\psi_2^1(0)$ unless the system is unreasonably forced to evolve starting from the unstable equilibrium point $\mathbf{x}_1$ by setting $\psi_1^1(0) = 1$. This is evident in Fig. 5, which shows the phase portrait of the proposed strategy for $k = 1/2 \in (0, 1/\sqrt{2}]$. Specifically, each curve in Fig. 5 represents the time evolution of the system in terms of the state variables (ψ_1^1, ψ_2^1), with the arrow denoting the direction of the evolution and the color depending on the norm of the vector field, i.e., the speed of the evolution.

2) $k \in (1/\sqrt{2}, 1] \iff q_2^1/\sqrt{2} < q_1^1 \leq q_2^1$: The evolution of the system depends on the initial conditions $\psi_1^1(0)$ and $\psi_2^1(0)$, as shown in Fig. 6. Specifically, since we have two asymptotically stable equilibrium points $\mathbf{x}_0$ and $\mathbf{x}_1$, the admissible state region $0 \leq \psi_1^1(t) + \psi_2^1(t) \leq 1$ is split in two separate subregions, divided by a curve passing through $\mathbf{x}_2(k)$. For any initial conditions belonging to the left subregion, the largest one, the system evolves toward $\mathbf{x}_0$, as shown by the gray trajectory in Fig. 6. Differently, for any initial conditions belonging to the right subregion, the smallest one, the system evolves toward $\mathbf{x}_1$, as shown by the black trajectory in Fig. 6. Clearly, when the channel qualities are comparable, the two subregions become comparable as well, as shown by Fig. 7 with $k = q_1^1/q_2^1 = 1$. Finally, for any initial conditions placed on the border between the two sub-regions, the system evolves toward the saddle point $\mathbf{x}_2(k)$. However, this case is not of any practical interest since, even if the initial conditions are chosen randomly, the event of having initial conditions placed on the border occurs with a negligible probability.

Remark. In a nutshell, whenever $0 < q_1^1 \leq \frac{q_2^1}{\sqrt{2}}$, i.e., whenever there exist a clear difference in terms of quality between the two available channels, the strategy assures the optimal spectrum allocation represented by $\mathbf{x}_0$ for any setting of the initial conditions. Differently, whenever $\frac{q_2^1}{\sqrt{2}} < q_1^1 \leq q_2^1$, i.e., whenever the channel qualities become comparable, the strategy is able to select the optimal allocation represented by $\mathbf{x}_0$ if the initial conditions are properly chosen, i.e., if $\psi_1^1(0) < x_1^1(k)$ and $\psi_2^1(0) \geq x_2^1(k)$ with $x_1^1(k)$ and $x_2^1(k)$ given in (8). It is worthwhile to note that $x_1^1(k)$ and $x_2^1(k)$ are univocally determined by the value of $k = \frac{q_1^1}{q_2^1}$, i.e., by the ratio between the two channel qualities. Hence, since as described in Sec. V these qualities can be easily estimated by the HN, the strategy is able to assure the optimal spectrum allocation in any case.

C. Scenario 2: Two Networks

We consider now the case of two HNs and two available Sub-6 GHz channels, with $q_1^1 \leq q_2^1 = q_1^2 = q_2^2$. This setting models the following scenario of practical interest: i) both the 1st and the 2nd channels are equally preferred by the 2nd HN; and ii) the 2nd channel is the preferred choice for the 1st HN. According to Def. 6, the optimal spectrum allocation is the one assuring the 1st HN fully committed to the 2nd channel and the 2nd HN fully committed to the 1st channel, i.e., $\tilde{\mathbf{x}} = (x_1^1, x_2^1, x_1^2, x_2^2) = (0, 1, 1, 0)$. By defining $k \triangleq q_1^1/q_2^1$,

This article has been accepted for publication in a future issue of this journal, but has not been fully edited. Content may change prior to final publication. Citation information: DOI 10.1109/TWC.2018.2864734, IEEE Transactions on Wireless Communications

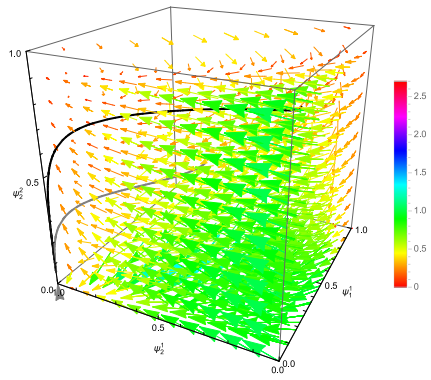

Fig. 8. Scenario 2: 3D-phase portrait for $k = 1/4$. Grey and black trajectories starting from with initial conditions $(0.4, 0.5, 0.3, 0.5)$ and $(0.7, 0.2, 0.2, 0.7)$, respectively.

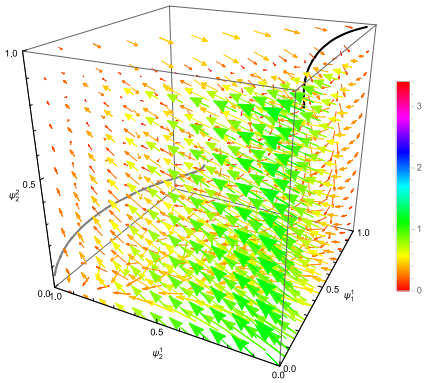

Fig. 9. Scenario 2: 3D-phase portrait for $k = 6/10$. Grey and black trajectories starting from with initial conditions $(0.4, 0.5, 0.3, 0.5)$ and $(0.7, 0.2, 0.2, 0.7)$, respectively.

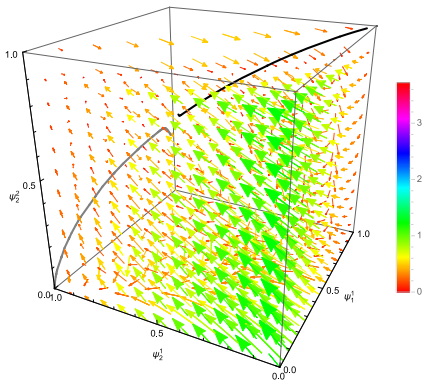

Fig. 10. Scenario 2: 3D-phase portrait for $k = 3/4$. Grey and black trajectory starting from initial conditions in the ϵ-neighborhood of $\mathbf{x}_5$.

the following results hold.

Lemma 2. ***(Equilibria)*** *The set E of the equilibrium points of the proposed strategy is:*

$$E = \begin{cases} \{\mathbf{x}_0, \mathbf{x}_1, \mathbf{x}_2, \mathbf{x}_3\} & \text{if } k \in (0, \frac{\sqrt{3}-1}{2}] \\ \{\mathbf{x}_0, \mathbf{x}_1, \mathbf{x}_2, \mathbf{x}_3, \mathbf{x}_4(k)\} & \text{if } k \in (\frac{\sqrt{3}-1}{2}, \frac{\sqrt{5}-1}{2}) \\ \{\mathbf{x}_0, \mathbf{x}_1, \mathbf{x}_2, \mathbf{x}_3\} & \text{if } k \in [\frac{\sqrt{5}-1}{2}, 1] \\ \{\mathbf{x}_5(k)\} & \text{if } k \in (k_0, 1] \end{cases} \quad (9)$$

with k_0 being the positive real radix of $\sqrt{3 - 7k^2 - 6k^3 + k^5}$. Specifically, we have $\mathbf{x}_0 = (0, 1, 1, 0)$, $\mathbf{x}_1 = (1, 0, 0, 1)$, $\mathbf{x}_2 = (0, 1, 0, 1)$, $\mathbf{x}_3 = (1, 0, 1, 0)$, $\mathbf{x}_4(k) = \big(x_1^1(k), x_2^1(k), x_1^2(k), x_2^2(k)\big)$ shown in Fig. 3 with $x_1^2(k) = 0$, $x_2^2(k) = 1$, $x_1^1(k)$ and $x_2^1(k)$ equal to:

$$x_1^1(k) = -1 + \frac{1}{2k} + \frac{1}{2}\sqrt{\frac{(k-1)^2}{k^2(k+1)^2}}$$
$$x_2^1(k) = \frac{k^2(x_1^1(k)^2 - 1)}{-k^2 - kx_1^1(k) - k^2 x_1^1(k)} \quad (10)$$

and, finally, $\mathbf{x}_5(k)$ shown in Fig. 4 for the sake of brevity.

Proof: See Appendix C ■

Remark. Similarly to Sec. IV-B, we have the valuable result of E composed by four regions depending on the value of $k \triangleq q_1^1/q_2^1$, i.e., the equilibria do not depend on the individual values of q_1^1 and q_2^1 but rather on the ratio between the two values. Furthermore, the equilibrium point $\mathbf{x}_0$ represents the optimal spectrum allocation $\tilde{\mathbf{x}}$ according to Def. 6. Indeed: i) there exists a consensus, i.e., all the agents are committed to the same channel; ii) the HNs do not overlap, i.e., different networks are committed to different channels and hence the coexistence interference is null ($I_c^n(\mathbf{x}_0) = 0$ when $1_c^n(\mathbf{x}_0) = 1$); iii) each HN is committed to the highest-quality channel. Differently, $\mathbf{x}_1$ represents a suboptimal spectrum allocation since there exists a full non-overlapping consensus, but the 1st network is not committed to the highest-quality channel—unless $k = 1$, when both $\mathbf{x}_0$ and $\mathbf{x}_1$ represent optimal allocations. Both $\mathbf{x}_2$ and $\mathbf{x}_3$ represent undesirable spectrum allocations, since the two HNs overlap, causing so a notable performance degradation. According to Def. 5, $\mathbf{x}_4$ represents an invalid spectrum allocation, since the 2nd HN is fully committed to the 2nd channel but the 1st HN experiences a partial commitment, with ratios significantly varying with k as shown in Fig. 3. Finally, $\mathbf{x}_5$ represents an invalid spectrum allocation as well, since both the HNs experience a partial commitment, with ratios slightly changing with k as shown in Fig. 4.

Proposition 2. ***(Stability)*** *$\mathbf{x}_0$ is an asymptotically stable equilibrium point for any $k \in (0, 1]$. Differently, $\mathbf{x}_1$ is an asymptotically stable equilibrium point for any $k \in (\frac{\sqrt{3}-1}{2}, 1]$, and an unstable equilibrium point for any $k \in (0, \frac{\sqrt{3}-1}{2}]$. Finally, the remaining equilibrium points are all unstable, being $\mathbf{x}_2$, $\mathbf{x}_3$, $\mathbf{x}_4(k)$ and $\mathbf{x}_5$ saddle points.*

Proof: See Appendix D ■

Stemming from these results, we have two cases.

1) $k \in (0, (\sqrt{3}-1)/2] \iff 0 < q_1^1 \leq q_2^1(\sqrt{3}-1)/2$: The system always evolves toward $\mathbf{x}_0$, i.e., the optimal spectrum allocation $\tilde{\mathbf{x}}$, regardless of the initial conditions $\{\psi_c^n(0)\}_{c=1,2}^{n=1,2}$ unless the system is unreasonably forced to evolve starting from one of the unstable equilibrium points $\mathbf{x}_1$, $\mathbf{x}_2$ or $\mathbf{x}_3$. This is evident in Fig. 8, which shows the 3-dimensional $(\psi_1^1, \psi_2^1, \psi_2^2)$-phase portrait — i.e., a 3-dimensional projection of the 4-dimensional system-phase portrait for the sake of practical representation — of the system for $k = 1/4 \in (0, \frac{\sqrt{3}-1}{2}]$. Specifically, each trajectory in Fig. 8 represents the time evolution of the system in terms of the state variables $(\psi_1^1, \psi_2^1, \psi_2^2)$, with the arrow denoting the direction of the evolution and the color depending on the norm of the vector field, i.e., the speed of the evolution. For any initial conditions different from the unstable equilibrium points $\mathbf{x}_1$, $\mathbf{x}_2$ and $\mathbf{x}_3$, the system evolves toward $\mathbf{x}_0$, as shown by both the gray and the black trajectories. This is confirmed by the direction of the arrows, toward 0 along ψ_1^1 and ψ_2^2, and toward 1 along ψ_2^1.

2) $k \in ((\sqrt{3}-1)/2, 1] \iff q_2^1(\sqrt{3}-1)/2 < q_1^1 \leq q_2^1$: The evolution of the system depends on the initial conditions, as shown by Fig. 9. Specifically, since we have two asymptotically stable equilibrium points $\mathbf{x}_0$ and $\mathbf{x}_1$, the admissible state region is split in two separate subregions. For any initial

This article has been accepted for publication in a future issue of this journal, but has not been fully edited. Content may change prior to final publication. Citation information: DOI 10.1109/TWC.2018.2864734, IEEE Transactions on Wireless Communications

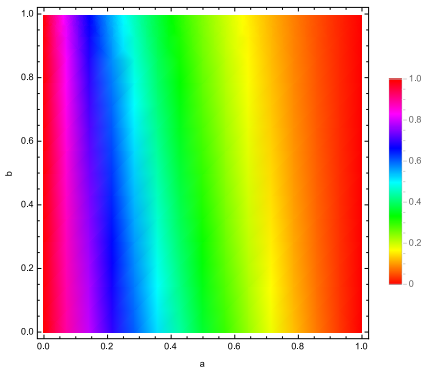

Fig. 11. Scenario 3: value of x_c^n as function of the inhibition factors $a > 0$ and $b < 1$.

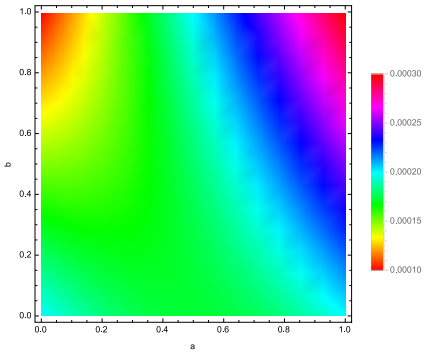

Fig. 12. Scenario 3: value of $\dot{\psi_c^n}(t)$ when $\psi_c^n(t) \rightarrow (x_c^n)^-$ as function of the inhibition factors $a > 0$ and $b < 1$.

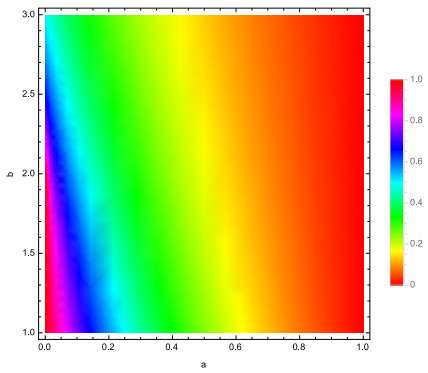

Fig. 13. Scenario 3: value of x_c^n as function of the inhibition factors $a \neq 0$ and $b > 1$.

conditions belonging to the first subregion, the system evolves toward the optimal spectrum allocation $\mathbf{x}_0$, as shown by the gray trajectory in Fig. 9. Differently, for any initial conditions belonging to the second subregion, the system evolves toward $\mathbf{x}_1$, as shown by the black trajectory in Fig. 9. Finally, there exist other four unstable equilibrium points, i.e., $\mathbf{x}_2$, $\mathbf{x}_3$, $\mathbf{x}_4(k)$ and $\mathbf{x}_5(k)$. However, they represent spectrum allocations of no practical interest since, even if the initial conditions are chosen randomly, the event of having the initial conditions placed in their regions of attraction occurs with a negligible probability. This is confirmed by Fig. 10, showing that the system evolves toward either $\mathbf{x}_0$ or $\mathbf{x}_1$, even when the initial conditions are placed within the ϵ-neighborhoods of the unstable equilibrium point $\mathbf{x}_5(k)$ when $k = 3/4$.

Remark. In a nutshell, whenever $0 < q_1^1 \leq q_2^1(\sqrt{3}-1)/2$, i.e., whenever there exist a clear difference in terms of quality between the two available channels, the strategy assures the optimal spectrum allocation represented by $\mathbf{x}_0$ for any setting of the initial conditions. Differently, whenever $q_2^1(\sqrt{3}-1)/2 < q_1^1 \leq q_2^1$, i.e., whenever the channel qualities become comparable, the strategy is able to select the optimal spectrum allocation represented by $\mathbf{x}_0$ if the initial conditions are properly chosen. However, the initial conditions depend on the number of networks coexisting in a given network region. Hence, since our proposal is completely blind with respect to any a-priori information, we chose the initial conditions at random. Nevertheless, since the volume of the homogeneous-trajectory subregions depend on the network preferences, the random choice of the initial conditions assures the selection of the optimal spectrum allocation with high probability. This valuable result is confirmed in Sec. VI-B with Fig. 15-B, showing that the probability of selecting the optimal spectrum allocation exceed 0.95. Clearly, if some a-priori information is available, a proper choice of the initial conditions can be made. However, we believe that the capability of our proposal to converge towards the optimal spectrum allocation without any a-priori information is a valuable feature of our proposal.

D. Scenario 3: General Case

Finally, we consider the generic case of N HNs accessing C Sub-6 GHz channels. The analysis of such a large system of coupled ODEs is particularly challenging and closed-form expressions of all the components of the equilibria cannot be derived. We anyway address this general case by looking at the local dynamics for the fraction of agents of the generic n-th network committed to the arbitrary c-th channel described by the following differential equation:

$$\dot{\psi_c^n}(t) = q_c^n(1-\psi_c^n(t)-a)\,(1+\psi_c^n(t)) - a\psi_c^n(t) + \\ -\psi_c^n(t)(1-\psi_c^n(t))\frac{b}{q_c^n} \tag{11}$$

with $a = \sum_{i\neq c}\psi_i^n(t) \in [0,1]$ and $b = \sum_{m\neq n}\psi_c^m(t) > 0$ denoting the overall intra- and inter-population dynamics. In a nutshell, a denotes the overall effect of the nodes of the same population committed to different channels trying to force the nodes committed to c-th channel to change their decision. Differently, b denotes the overall effect of the nodes of different populations committed to the same channel trying to force the nodes committed to c-th channel to change their decision. Hence, a represents the *internal* force toward a different decision, whereas b represents the *external* force toward a different decision.

By setting $q_c^n = 1$, we have that the c-th channel is an ideal channel for the n-th HNs.

Lemma 3. ***(Equilibrium Points)*** *The set E of the ψ_c^n-coordinate at the equilibrium is given by:*

$$E = \begin{cases} \{x_c^n = \frac{2a+b}{2(b-1)} + z\} & \text{if } a > 0 \wedge b < 1 \\ \{x_c^n = \frac{1-a}{1+2a}\} & \text{if } a > 0 \wedge b = 1 \\ \{x_c^n = \frac{2a+b}{2(b-1)} - z\} & \text{if } a > 0 \wedge b > 1 \\ \{x_c^n = 1\} & \text{if } a = 0 \end{cases} \tag{12}$$

with $z = \sqrt{\frac{4-4a+4a^2-4b+8ab+b^2}{4(b-1)^2}}$.

Proof: See Appendix E ■

We discuss now the results of Lemma 3. In Fig. 11, we report the value of the equilibrium x_c^n as function of both the inhibition factors $a \neq 0$ and $b < 1$. We observe that, the value of x_c^n mainly depends on a, i.e., the intra-population inhibition. To analyze the stability of x_c^n, we must look at the sign of (11), and it results that the system always evolves toward x_c^n. In fact, whenever $a > 0$ and $0 \leq b < 1$ we obtain $\dot{\psi_c^n}(t) < 0 \iff \psi_c^n(t) > x_c^n$ and $\dot{\psi_c^n}(t) > 0 \iff \psi_c^n(t) < x_c^n$.

This article has been accepted for publication in a future issue of this journal, but has not been fully edited. Content may change prior to final publication. Citation information: DOI 10.1109/TWC.2018.2864734, IEEE Transactions on Wireless Communications

This result is confirmed by Fig. 12, which shows the sign of $\dot{\psi}_c^n(t)$ when $\psi_c^n(t)$ approaches x_c^n from left as a function of a and b. Differently, when $b > 1$, as depicted in Fig. 13, we observe that the value of x_c^n depends on both a and b. Specifically, the value decreases with b, i.e., it decreases as the number of agents belonging to a different population and committed to channel c increases. As regards to the system evolution, we have that x_c^n represents an attractor for the ψ_c^n-coordinate. Similar results hold for the other conditions when $b = 1$, while the special case $a = 0$ corresponds to the n-th HN fully committed to channel c.

Remark. In a nutshell, whenever $b < 1$, the population dynamics mainly depend on the intra-population dynamics, whereas whenever $b \geq 1$ the population dynamics depend also on the inter-population dynamics. Since closed-form expressions of all the components of the equilibria cannot be derived, a rigorous stability analysis can not be conducted. However, we are able to show through simulations that the random choice of the initial conditions assures the selection of the optimal allocation with high probability (see Fig. 16 in Sec. VI-C). As pointed out in Sec. IV-D, although a proper choice of the initial conditions can be made when a-priori information is available, we believe that the capability to converge towards the optimal spectrum allocation without any a-priori information is a valuable feature of our proposal.

V. Strategy Discussion

A. Strategy Implementation

Here, we discuss some practical aspects for implementing the proposed strategy in a real-world scenario. As said, we focus on designing an *autonomous* and *fully-distributed* strategy. Hence, we aim at defining a strategy where:

i) the intra-population dynamics can evolve independently from each other through local interactions, i.e., through broadcast communications to neighbor nodes;
ii) the inter-population dynamics are driven by a process directly available to each HN, i.e., no direct communications among different HNs are required.
iii) the dynamics drive the system toward a convenient and fair solution, namely, a solution assigning to each HN a channel satisfying its communication needs by accounting for the coexistence interference.

Stemming from this, without loss of generality since the results derived through the paper can be easily extended to different channel quality metrics, we define the channel quality q_c^n as the 1-bounded ratio between the capacity ν_c^n achievable by the n-th HN over the c-th channel and the n-th network demand in terms of data-rate d^n, i.e.:

$$q_c^n = \min\left\{1, \frac{\nu_c^n}{d^n}\right\} \tag{13}$$

The rationale for the capacity normalization is to take into account that channels with different capacities can be equally preferable as long as they are able to accommodate the network demand. By substituting (13) in (3), we have that three (out of four) parameters piloting the commitment dynamics, i.e., the channel capacity ν_c^n, the average network demand d^n and the commitment ratio $\psi_c^n(t)$, can be easily computed at each HN through asynchronous broadcast messages to neighbor nodes [40], stemming from information (i.e., measured SNR and current agent's demand) locally available at each agent.

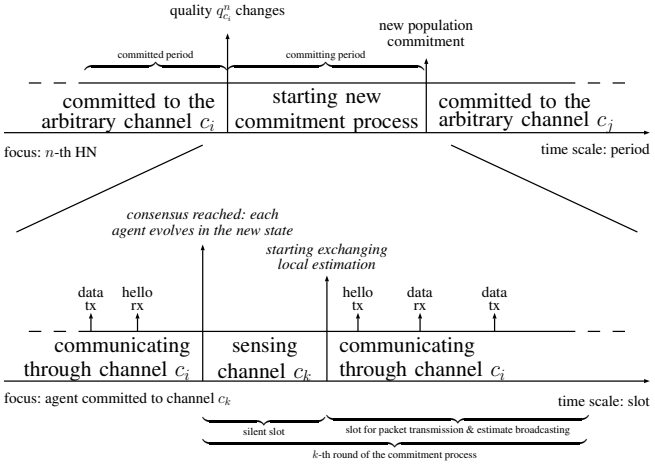

Fig. 14. Schematic illustration of the time structure of the n-th HN (above) and of the arbitrary agent belonging to the n-th HN and committed to the generic channel c_k (below). Time duration proportion among periods/slots not respected for the sake of clarity.

As regards to the fourth parameter piloting the commitment dynamics, i.e., the coexistence interference $\mathcal{I}_c^n(t)$, a possible estimation approach exploiting a dedicated *sensing slot* is described in the following. The time horizon of the n-th population is organized into a sequence of time periods, as shown in the upper plot of Fig. 14. Within a *committing period*, a channel, say channel c_i, is distributively and autonomously selected by the n-th HN, and during the subsequent *committed period* the selected channel is used for data-packet transmission. A new committing period starts whenever the previously selected channel c_i does not satisfy the n-th HN communication needs, as instance when the perceived coexistence interference increases.

Each *committing period* can be further decomposed into a sequence of *rounds* as shown by the lower plot of Fig. 14. Each round is organized into two time slots: a shorter *sensing slot* followed by a considerably longer *transmission slot*. Within the *sensing slot*, the n-th HN is silent (i.e., no communications occur within the n-th HN), allowing so any agent committed to a given channel, say channel c_k, to easily estimate the coexistence interference $\mathcal{I}_c^n(t)$ on such a channel by simply sensing the channel. Differently, during the subsequent *transmission slot*, data communications normally occur through the previously selected channel, i.e., channel c_i. Additionally, such a slot is also used to transmit the asynchronous broadcast messages for computing the parameters (ν_c^n, d^n, $\psi_c^n(t)$ and $\mathcal{I}_c^n(t)$) piloting the commitment dynamics. Clearly, at network initialization (during the first round of the first period) the channel is randomly selected.

This article has been accepted for publication in a future issue of this journal, but has not been fully edited. Content may change prior to final publication. Citation information: DOI 10.1109/TWC.2018.2864734, IEEE Transactions on Wireless Communications

B. Challenges and Open Problems

The design of an *autonomous* and *fully-distributed* strategy undoubtedly poses challenges and drawbacks, which we discuss in the following.

First, it is required that each HN remains silent during the sensing slot to properly estimate the magnitude of the interference $\mathcal{I}_c^n(t)$. This clearly affects the overall network throughput as well as the possible (real-)time constraints of the data traffic. Nevertheless, we believe that the advantage of avoiding inter-HN communications is worth to incurring in such a drawback. Furthermore, as extensively shown in the Cognitive Radio literature, the duration of these silent slots can be narrowed down to values in the order of few milliseconds every hundreds of milliseconds or more [41], with a negligible impact on the HN performance and making statistically unlikely the failure of the interference magnitude estimation due to multiple HNs simultaneously silent. Finally, by leveraging the latest Sub-6 GHz prototypes ability to simultaneously establish redundant links [4], it is possible to assure a seamless connectivity while sensing for the interference magnitude.

Another drawback is represented by the overhead due to the messages broadcasted to neighbor nodes for distributedly estimating the four parameters piloting the commitment dynamics, i.e., ν_c^n, d^n, $\psi_c^n(t)$, and $\mathcal{I}_c^n(t)$. This overhead is intrinsically related to the distributed feature of the designed strategy. However, as shown in Sec. VI, the convergence toward the optimal spectrum allocation is usually reached with a reasonable number of rounds, and the overhead can be further narrowed down by appending the local estimates within the control packets usually broadcasted at layer 2/3.

Furthermore, the commitment dynamics can be affected by the spatial distribution of nodes within a HN, especially when cellular networks or very large multi-hop networks are considered. Indeed, the design strategy, linking macroscopic dynamics to individual agent rules, we present here assumes a well-mixed system, whereby interactions among any node within the HN is equally likely. When this assumption does not hold, it is possible to implement specific measures to simulate a well-mixed condition as much as possible [19]. Current theoretical studies to deal with spatial heterogeneities at design time are under way [42], [43], and can be included in the proposed design strategy in future work.

Finally, another aspect to be considered is the capacity of the proposed strategy to converge towards a solution representing a full consensus among its nodes, given in Def. 5. Stemming from the analysis in [19], full consensus can be achieved only if the rate of a node to spontaneously abandon commitment is null, as there are no other mechanisms to change commitment state when a population is fully allocated on the same channel. In our design, the abandonment rate is null when either there is no interference or full consensus has already been achieved, as defined in (3). Hence, whenever abandonment remains non-null, for any reason (e.g., there are fewer channels than networks, hence some interference is always present, albeit small), a strategy to reach full consensus is required. As detailed in Sec. VI, we force full consensus by setting a null abandonment rate either after a maximum allotted time, or when a sufficiently high percentage of the population — referred to as "quorum" — is detected on the same channel. It is worth noting, however, that maintaining a non-null abandonment rate may be valuable, as it preserves a dynamic behavior of the nodes that can explore other alternatives as they become available.

VI. Performance Evaluation

Here, we validate the theoretical analysis and demonstrate the benefits provided by the designed strategy by implementing a multi-agent simulation that reproduces the dynamics discussed in Sec. III [19]. We considered two different strategy implementations. The *interference implementation* estimates $\mathcal{I}_c^n(t)$ as the average ratio of time during which the channel is interfered (see Sec. V). The *distribution implementation* estimates $\mathcal{I}_c^n(t)$ as the the sum of the fraction of nodes of different HNs committed to the same channel (see Sec. IV). By comparing the two implementations, we can obtain information about the validity of the theoretical analysis and the suitability of our design. Given that the proposed strategy may not lead to consensus when $\alpha_c^n(t)$ is not null, we introduce the quorum threshold θ^n: whenever $\exists c : \psi_c^n(t) > \theta^n$, the consensus on channel c is forced by setting the abandonment term $\alpha_c^n(t) = 0$. To evaluate the performance of the proposed strategies, we consider two performance metrics: (i) the *convergence time* t_c, i.e., the time required to achieve a stable allocation of HNs among the available channels; (ii) the *normalized overall quality* $d^\star = \mathcal{Q}(\mathbf{x})/\mathcal{Q}(\tilde{\mathbf{x}})$, denoting the ratio between the overall quality achieved by the spectrum allocation $\mathbf{x}$ obtained with the proposed strategy as from (6) and the overall quality achieved by the optimal spectrum allocation $\tilde{\mathbf{x}}$ as from Def. 6.

We compare the normalized overall quality $d^\star$ with the one obtained by two centralized greedy algorithms: the *best greedy* and the *proportional greedy*, denoted with d^b and d^p respectively. Both algorithms allow HNs to make a greedy selection of the channel that maximizes the expected quality, taking into account the coexistence interference on every available channel in $\mathcal{C}$ [34]. For comparison with our strategy, we assume that the channel selection process is iterated for a fixed number of rounds R within a committing period. In each round, each HN makes a centralized decision with probability μ, hence simulating the asynchronous and independent decisions made by HNs. With the best greedy strategy, each HN selects the channel that maximizes the expected quality. With the proportional greedy strategy, each HN selects a channel with probability proportional to its expected quality. After R rounds, the currently chosen allocation is selected. In this work, we set $\mu = 0.1$ and $R = 5000$.

Note that these centralized algorithms—being seamless although not self-organizing—allow us to conduct a fair performance comparison, also considering the lack of alternatives in the literature about seamless self-organizing coexistence strategies, as discussed in Sec. I-A. We further observe that in all the considered experiments we assume the challenging scenario of just two available channels. Indeed, the higher the number of channels, the higher the opportunities for

This article has been accepted for publication in a future issue of this journal, but has not been fully edited. Content may change prior to final publication. Citation information: DOI 10.1109/TWC.2018.2864734, IEEE Transactions on Wireless Communications

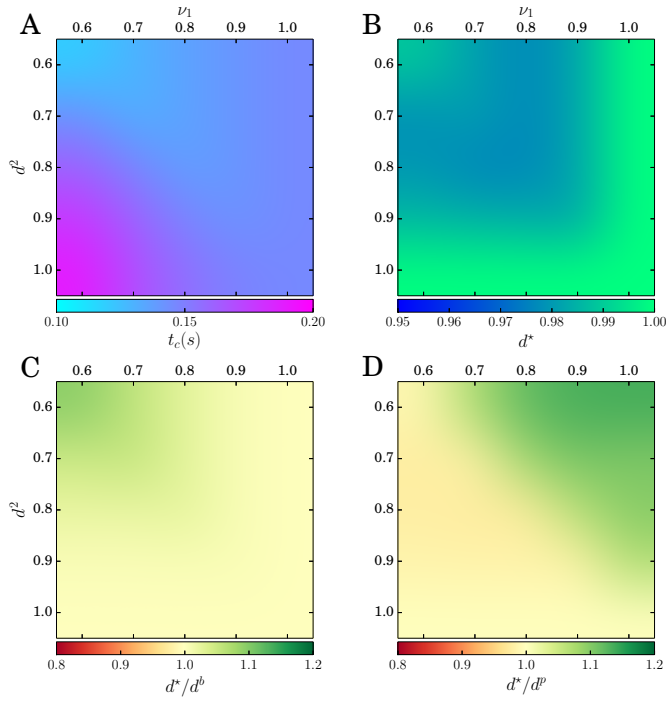

Fig. 15. Experiment 1. A: convergence time t_c. B: normalized overall quality $d^\star$. C: overall quality ratio $d^\star/d^b$ with respect to the best greedy strategy. D: overall quality ratio $d^\star/d^p$ with respect to the proportional greedy strategy.

coexistence at the price of longer convergences times [39], [44]. Moreover, in agreement with experimental studies (e.g., TV White Space [45]), the number of channels available for the opportunist spectrum access is generally limited to a few, especially in urban environments.

A. Experiment 1: two networks

Two HNs, each composed of 100 nodes, compete for two channels, c_1 with varying capacity $\nu_1 \in \{0.6, 0.7, 0.8, 0.9, 1\}$ and c_2 with fixed capacity $\nu_2 = 1$. One HN has fixed demand $d^1 = 1$, while the other has variable demand $d^2 \in \{0.6, 0.7, 0.8, 0.9, 1\}$. We obtain 25 different configurations and, for each, we compute average figures over 500 independent runs, setting the quorum threshold $\theta^n = 1$. Indeed, with two networks and two channels, it is always possible to have an interference-free allocation and the proposed strategy always reaches full consensus. The results are displayed in Fig. 15, where we display only the results obtained with the *distribution* implementation, those obtained with the *interference* implementation being very similar.

With the above setting, we can explore various experimental conditions. When $\nu_1 \geq d^2$, we have that $q_1^2 = 1$, hence we are in the conditions analyzed in Sect. IV-C with $k = q_1^1$. In such a case, we have for $k > \frac{\sqrt{3}-1}{2}$ the existence of a bi-stable regime with a suitable interference-free allocation that completely fulfills the demand, and a second suboptimal interference-free allocation (apart from the case $k = 1$ where both allocations are optimal). In particular, when $k = \frac{\sqrt{5}-1}{2} \approx 0.62$, the macroscopic analysis predicts a phase transition, hence we expect to see different behaviors around this value. Conversely, whenever $\nu_1 < d^2$, there is no allocation that completely satisfies the HNs demands. Nevertheless, the designed strategy is able to achieve consensus also in this case, although after a slightly longer time, as shown in Fig. 15-A. Indeed, fairly low values of the convergence time t_c are required (about 0.15s in average by assuming updates every $\tau = 1$ms), but a slightly longer time is needed when $\nu_1 < d^2$, suggesting that a convergence is more difficult in presence of sub-optimal conditions.

The normalized overall quality $d^\star$ is shown in Fig. 15-B. Here, we observe an optimal behavior for $\nu_1 = 1$ or $d^2 = 1$, corresponding to the symmetric condition with equivalent channels or identical demands, in which any interference-free allocation is good. The proposed strategy allows to break the symmetry in all these conditions. Elsewhere, we note a departure from optimality due to finite-size stochastic fluctuations, which bring the system in the basin of attraction of the sub-optimal stable point $\mathbf{x}_1$. Notably, we have a slightly higher performance for $\nu_1 = 0.6$ and $d^2 = 0.6$, which corresponds to $k = 0.6$. In this case, the additional unstable equilibrium point $\mathbf{x_4}(k)$ favors convergence to the optimal allocation. In any case, the error is always within 5% of the optimal allocation, with the minimum value $d^\star \simeq 0.97$ for $d^2 = 0.8$ and $\nu_1 = 0.7$. Finally, in Fig. 15-C and 15-D, we compare the proposed strategy with the two centralized greedy algorithms through the ratios $q^\star/q^b$ and $q^\star/q^p$, respectively. We note that the proposed strategy has the same or better performance in all configurations, with a larger advantage over the proportional greedy strategy when $\nu_1 > d^2$. Overall, these results confirm the appropriateness of the designed strategy and highlight the close match with the analytical results from Sec. IV-C.

B. Experiment 2: three networks

A more challenging scenario involves three HNs competing for two channels. Here, two HNs must share the same channel, hence interfering with each other, albeit minimally if the channel capacity is sufficiently large. We consider varying channel capacities and HN demands. The former are defined in the same way as in Sec. VI-A. The latter are defined as follows: $d^1 = 0.8$, $d^{2,3} = d^2 + d^3 \in \{0.6, 0.7, 0.8, 0.9, 1\}$ with $d^2/d^3 = 2/3$. Here, we use a threshold $\theta^n = 0.75$ for any n, to allow termination as abandonment is not null for those HNs that share the same channel. With Fig. 16, we provide results for both implementations, i.e., *distribution* and *interference*.

Results show that the proposed strategy presents good performance, featuring quick convergence and a good quality $d^\star$. Time-wise, the results for distribution clearly indicate that conditions where $\nu_1 > 0.8$ require a longer time to reach a good allocation ($> 0.3s$, see Fig. 16-A). In these conditions, the two channels have similar capacity and breaking the symmetry with three HNs appears slower. Similarly, the normalized overall quality is lower, as shown in Fig. 16-B. The situation is reversed for the interference implementation, which presents a shorter convergence time when $d^{2,3} < \nu_1$ (Fig. 16-E) and generally a better normalized quality than distribution (Fig. 16-F). This is because the distribution implementation is based on information about the fraction of other populations on the

This article has been accepted for publication in a future issue of this journal, but has not been fully edited. Content may change prior to final publication. Citation information: DOI 10.1109/TWC.2018.2864734, IEEE Transactions on Wireless Communications

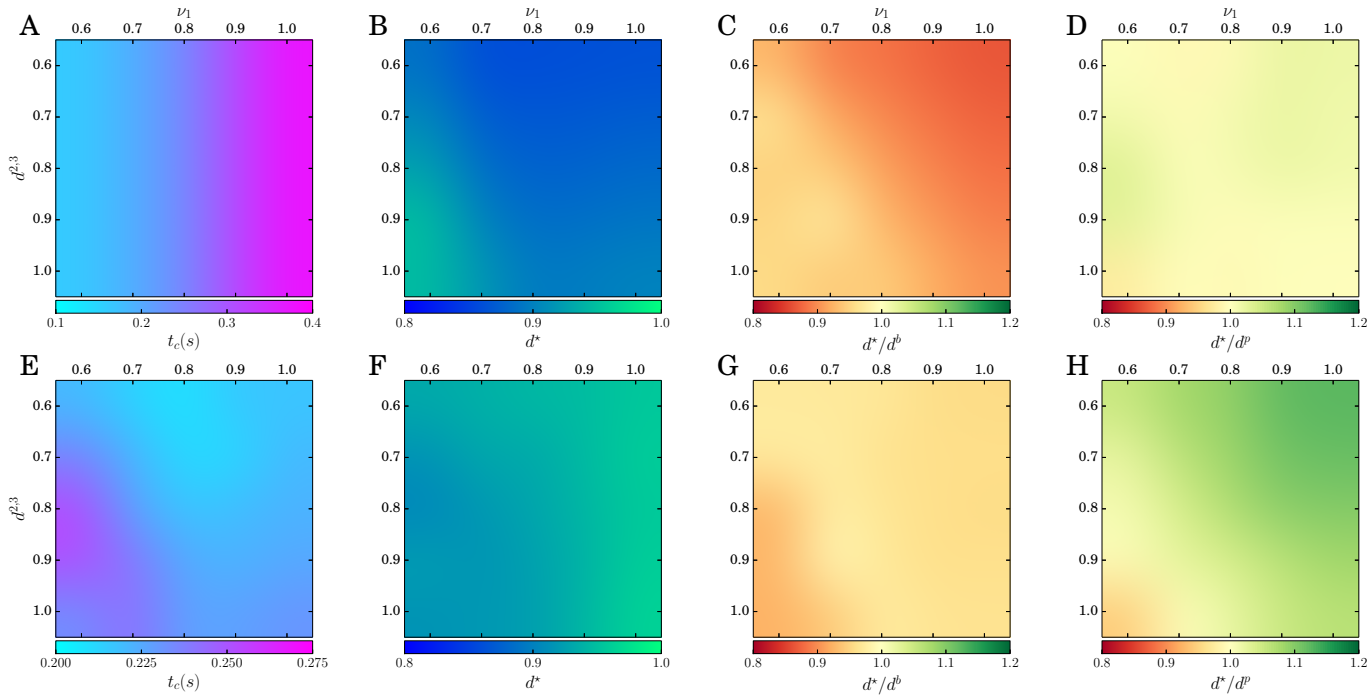

Fig. 16. Experiment 2. A-D: *distribution* implementation. E-H: *interference* implementation. A,E: convergence time t_c. B,F: normalized overall quality $d^\star$. Comparison with the best greedy (C,G) and the proportional greedy strategy (D,H).

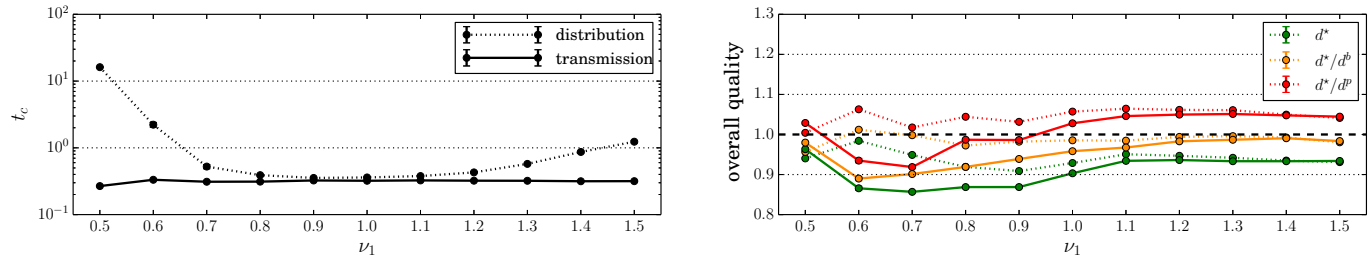

Fig. 17. Experiment 3. Left: convergence time t_c. Right: normalized overall quality ($d^\star$) and quality relative to the centralized greedy strategies, best and proportional ($d^\star/d^b$ and $d^\star/d^p$). Error-bars are too small to be visible on the scale of the plot.

channel they occupy, which can overestimate the interference that they may produce. Specifically, by correctly estimating the interference among HNs on the same channel, it is possible to obtain a lower convergence time ($t_c \approx 0.22$s in average for interference vs. $tc \approx 0.25$s for distribution), a better allocation of the HNs ($d^\star \approx 0.94$ for interference vs $d^\star \approx 0.89$ for distribution). The comparison with the centralized strategies is also shown in Fig. 16. We note that in this more complex problem, the best greedy strategy achieves slightly better results than the decentralized strategies, with $d^\star/d^b \approx 0.92$ and $d^\star/d^b \approx 0.96$ (see panels C and G in Fig. 16). The proportional greedy strategy, instead, is generally outperformed by our decentralized designs (see panels D and H in Fig. 16). It is worth noting, however, that such a small advantage for the best greedy strategy is based on the aggregated knowledge of the interference expected on each available channel, which is a rather costly assumption that does not affect our strategies, which, being decentralized, can rely on the interference that each node individually senses on the channel it is committed to.

C. Experiment 3: five networks

Here, we consider a crowded scenario where five HNs compete for two channels. We consider HNs with fixed demand: $d^i = 0.2i - 0.1, i = 1, \ldots, 5$, with a total demand $d^t = \sum_i d^i = 2.5$. We consider one channel with varying capacity $\nu_1 \in \{0.5, \ldots, 1.5\}$ and a second channel with fixed capacity $\nu_2 = 1.5$, so that the total capacity can be either lower or higher than the total demand. We plot the results in Fig. 17. In the left panel, we show the differences in terms of t_c for the two implementations with a log-scale on the y-axis, and similar considerations of Sec. VI-B hold. Specifically, the *interference* implementation leads to roughly constant convergence times for the various experimental configurations ($t_c \simeq 0.3$s on average).

The normalized overall quality of the proposed strategy is also good, being in average $d^\star \approx 0.94$ for distribution and $d^\star \approx 0.9$ for interference. We note here that distribution

This article has been accepted for publication in a future issue of this journal, but has not been fully edited. Content may change prior to final publication. Citation information: DOI 10.1109/TWC.2018.2864734, IEEE Transactions on Wireless Communications

performs slightly better than transmission. This is because with this crowded setup, there is always interference perceived on both channels, and therefore the transmission implementation has more difficulties in choosing the optimal allocation with respect to the distribution implementation, which instead can rely on the detailed information about the fraction of nodes of other networks. This has importance especially when the total capacity of the two channels is lower than the total demand ($\nu_1 < 1$), implying that a strong interference is present. The comparison with respect to the centralized greedy strategies presents a similar picture as in Sec. VI-B, with the greedy best strategy performing slightly better—although with a small advantage—and the greedy proportional strategy being often worse than the decentralized strategies.

VII. Conclusions

In this paper, we proposed a self-organizing strategy to minimize the coexistence interference among heterogeneous networks operating in the Sub-6 GHz spectrum. The proposed strategy jointly promotes a selfless network utilization of the spectrum and avoids any direct communication among the heterogeneous networks. Specifically, we developed an analytical framework grounded on the nest-site selection behavior observed in honeybee swarms to model the coexistence problem among multiple heterogeneous unlicensed networks. We analytically studied the equilibria of the proposed strategy, and we derived the conditions for the strategy to guarantee an optimal spectrum allocation, i.e., the spectrum allocation minimizing the coexistence interference. The proposed strategy has been validated through an extensive performance evaluation, which confirmed the close match between analytical results and multi-agent simulations, suggesting that the proposed approach for the design of a self-organizing strategy is viable.

Appendix A
Proof of Lemma 1

The decision process time-evolution is described by the following bi-dimensional system:

$$\begin{aligned}\dot{\psi}_1^1(t) &= q_1^1\,\psi_u^1(t)\left(1+\psi_1^1(t)\right) - q_2^1\psi_1^1(t)\psi_2^1(t)\\ \dot{\psi}_2^1(t) &= q_2^1\,\psi_u^1(t)\left(1+\psi_2^1(t)\right) - q_1^1\psi_1^2(t)\psi_1^1(t)\end{aligned} \tag{14}$$

with $\psi_1^1(0)$ and $\psi_2^1(0)$ denoting the initial conditions. Note that the lack of interference from additional HNs leads to a null abandonment rate. By substituting (2) in (14), we obtain:

$$\begin{aligned}\dot{\psi_1^1} &= q_1^1(1-\psi_1^1-\psi_2^1)\left(1+\psi_1^1\right) - q_2^1\psi_1^1\psi_2^1\\ \dot{\psi_2^1} &= q_2^1(1-\psi_1^1-\psi_2^1)\left(1+\psi_2^1\right) - q_1^1\psi_1^1\psi_2^1\end{aligned} \tag{15}$$

where we omit the time dependence for the sake of notation simplicity. According to Def. 3, any equilibrium point $\mathbf{x}$ is a constant solution of the differential equations in (15). Hence, by imposing $\dot{\psi}_1^1$ and $\dot{\psi}_2^1$ equal to zero and by accounting for the definition of k, from (15) we obtain:

$$\begin{aligned}k(1-\psi_1^1-\psi_2^1)\left(1+\psi_1^1\right) - \psi_1^1\psi_2^1 = 0\\ (1-\psi_1^1-\psi_2^1)\left(1+\psi_2^1\right) - k\psi_1^1\psi_2^1 = 0\end{aligned} \tag{16}$$

and, after some algebraic manipulations, we derive the equilibria set E given in (7).

Appendix B
Proof of Proposition 1

To analyze the stability of each equilibrium point, we first derive the expression of the Jacobian matrix $J \triangleq \left(\frac{1}{q_2^1}\frac{\partial\dot{\psi}_i^1}{\partial\psi_j^1}\right)_{i,j\in\mathcal{C}}$ with $\frac{1}{q_2^1}$ positive normalizing factor and $k \triangleq q_1^1/q_2^1$:

$$J = \begin{pmatrix} -\psi_2^1 - k(2\psi_1^1+\psi_2^1) & -\psi_1^1 - k(1+\psi_1^1)\\ -1-(1+k)\psi_2^1 & -(1+k)\psi_1^1 - 2\psi_2^1\end{pmatrix} \tag{17}$$

Then, we assess the eigenvalues of J at the equilibrium points given in (7) by deriving the values of λ satisfying the equation $|J(\mathbf{x}) - \lambda I| = 0$. As regards to $\mathbf{x}_0$, the set $\sigma_{J(\mathbf{x}_0)}$ of eigenvalues is $\sigma_{J(\mathbf{x}_0)} = \left\{-(k+3\pm\sqrt{(k+1)(5k+1)})/2\right\}$ with both the eigenvalues real negative for any $k \in (0,1]$. Hence, $\mathbf{x}_0$ is an asymptotically stable equilibrium point. As regards to $\mathbf{x}_1$, the set $\sigma_{J(\mathbf{x}_1)}$ is $\sigma_{J(\mathbf{x}_1)} = \left\{-(3k+1\pm\sqrt{(k+1)(k+5)})/2\right\}$ with one eigenvalue real negative for any $k \in (0,1]$ and the other eigenvalue real negative for $k \in (1/\sqrt{2},1]$ and non-negative for $k \in (0,1/\sqrt{2}]$. Hence, $\mathbf{x}_1$ is an asymptotically stable equilibrium point when $k \in (1/\sqrt{2},1]$, and a saddle point (i.e., unstable equilibrium point) otherwise. Similarly, as regards to $\mathbf{x}_2(k)$, we have one eigenvalue real negative for any $k \in (1/\sqrt{2},1]$ and the other eigenvalue real positive for any $k \in (1/\sqrt{2},1]$. Hence, $\mathbf{x}_2$ is a saddle point for any $k \in (1/\sqrt{2},1]$.

Appendix C
Proof of Lemma 2

The time-evolution of the decision process is described by the following 4-dimensional system:

$$\begin{aligned}\dot{\psi_c^n}(t) =& q_c^n\,\psi_u^n(t)\,(1+\psi_c^n(t)) - q_{\bar{c}}^n\psi_c^n(t)\psi_{\bar{c}}^n(t) +\\ &- \frac{\psi_c^n(t)}{q_c^n}(1-\psi_c^n(t))\psi_c^{\bar{n}}(t)), \quad c,n\in\{1,2\}\end{aligned} \tag{18}$$

with the operator $\bar{(\cdot)}$ defined as $\bar{x}=2$ if $x=1$, $\bar{x}=1$ otherwise. By substituting (2) in (18) and after some algebraic manipulations, we derive the equilibria set E given in (9).

Appendix D
Proof of Proposition 2

To analyze the stability of each equilibrium point, we first derive in (19) shown in the next page the expression of the Jacobian matrix $J \triangleq \left(\frac{1}{q_2^1}\frac{\partial\dot{\psi}_i^l}{\partial\psi_j^m}\right)_{i,j\in\mathcal{C}}^{l,m\in\mathcal{N}}$ with $\frac{1}{q_2^1}$ positive normalizing factor and $k \triangleq q_1^1/q_2^1$.

Then, we assess the eigenvalues of J at the equilibrium points given in (9) by deriving the values of λ satisfying the equation $|J(\mathbf{x}) - \lambda I| = 0$. As regards to $\mathbf{x}_0$, the set $\sigma_{J(\mathbf{x}_0)}$ of eigenvalues is constituted by $(-5\pm\sqrt{13})/2$ and $(-1-3k-k^2\pm\sqrt{1-2k+3k^2+6k^3+5k^4}/2k$ with both the eigenvalues negative for any $k\in(0,1]$. Hence, $\mathbf{x}_0$ is an asymptotically stable equilibrium point. As regards to $\mathbf{x}_1$, the set $\sigma_{J(\mathbf{x}_1)}$ is $\sigma_{J(\mathbf{x}_1)} = \left\{(-5\pm\sqrt{13})/2, (-2-3k\pm\sqrt{8+4k+k^2})/2\right\}$ with tree eigenvalues negative for any $k\in(0,1]$ and one eigenvalue negative for $k\in(\frac{\sqrt{3}-1}{2},1]$ and non-negative for $k\in$

$$J = \begin{pmatrix} \frac{\psi_1^2}{k}(-1+2\psi_1^1)-(\psi_2^1+k(2\psi_1^1+\psi_2^1)) & -\psi_1^1-k(1+\psi_1^1) & \frac{\psi_1^1}{k}(-1+\psi_1^1) & 0 \\ -1-(1+k)\psi_2^1 & -(1+k)\psi_1^1+2\psi_2^1(-1+\psi_2^2)-\psi_2^2 & 0 & (-1+\psi_2^1)\psi_2^1 \\ (-1+\psi_1^2)\psi_1^2 & 0 & 2\psi_1^2(-1+\psi_1^1)-\psi_1^1-2\psi_2^2 & -1-2\psi_2^1 \\ 0 & (-1+\psi_2^2)\psi_2^2 & -1-2\psi_2^2 & -2\psi_1^2-\psi_2^1+2(-1+\psi_2^1)\psi_2^2 \end{pmatrix} \quad (19)$$

$(0, \frac{\sqrt{3}-1}{2}]$. Hence, $\mathbf{x}_1$ is an asymptotically stable equilibrium point when $k \in (\frac{\sqrt{3}-1}{2}, 1]$, and a saddle point (i.e., unstable equilibrium point) otherwise. As regards to $\mathbf{x}_2$, the set $\sigma_{J(\mathbf{x}_2)}$ is $\sigma_{J(\mathbf{x}_2)} = \left\{(-3 \pm \sqrt{13})/2, (-2-k \pm \sqrt{k}\sqrt{8+5k})/2\right\}$ with two eigenvalues negative for any $k \in (0, 1]$, one eigenvalue positive for any $k \in (0, 1]$ and one eigenvalue negative for $k \in (\frac{\sqrt{5}-1}{2}, 1]$ and non-negative for $k \in (0, \frac{\sqrt{5}-1}{2}]$. Hence, $\mathbf{x}_2$ is a saddle point for any $k \in (0, 1]$. Similarly, it results $\sigma_{J(\mathbf{x}_3)}$ constituted by $(-3 \pm \sqrt{13})/2$ and $(1-k-3k^2 \pm \sqrt{1+2k+3k^2+6k^3+k^4})/2k$ with two eigenvalues negative for any $k \in (0, 1]$ and two eigenvalues positive for any $k \in (0, 1]$. Hence, $\mathbf{x}_3$ is a saddle point for any $k \in (0, 1]$. As regards to $\mathbf{x}_4(k)$, we do not report the set $\sigma_{J(\mathbf{x}_4(k))}$ for the sake of brevity. However, we have at least one eigenvalue positive for any $k \in (\frac{\sqrt{3}-1}{2}, \frac{\sqrt{5}-1}{2})$. Hence, $\mathbf{x}_4(k)$ is a saddle point for any $k \in (\frac{\sqrt{3}-1}{2}, \frac{\sqrt{5}-1}{2})$. Similarly, $\mathbf{x}_5(k)$ is a a saddle point for any $k \in (k_0, 1]$.

APPENDIX E
PROOF OF LEMMA 3

The time-evolution of the decision process for the fraction of agents of the generic n-th network committed to the arbitrary c-th channel is given in (11). After some algebraic manipulations and by setting $z = \sqrt{\frac{4-4a+4a^2-4b+8ab+b^2}{4(b-1)^2}}$, we derive the set E of the equilibrium points given in (12).

REFERENCES

[1] V. Trianni, A. S. Cacciapuoti, and M. Caleffi, "Distributed Design for Fair Coexistence in TVWS," in *Proc. of IEEE ICC*, 2016.

[2] Z. Khan *et al.*, "On opportunistic spectrum access in radar bands: Lessons learned from measurement of weather radar signals," *IEEE Wireless Communications*, vol. 23, no. 3, pp. 40–48, June 2016.

[3] GSM Association, "5G Spectrum Public Policy Position," Tech. Rep., Nov. 2016.

[4] I. Qualcomm Technologies, "Making 5G NR a reality," White Paper, Dec. 2016.

[5] J. Li, X. Wang *et al.*, "Share in the Commons: Coexistence between LTE Unlicensed and Wi-Fi," *IEEE Wireless Communications*, vol. 23, no. 6, pp. 16–23, Dec. 2016.

[6] H. T. Co. World's First Sub-6GHz 5G Test Bed. [Online]. Available: http://www.huawei.com/minisite/5g/en/fist-sub-6ghz-5g.html

[7] I. Qualcomm Technologies. (2016, June) Qualcomm announces 5G NR sub-6 GHz prototype system and trial platform. [Online]. Available: https://www.qualcomm.com/news/releases

[8] Intel Corporation. (2017, Jan.) Intel Accelerates the Future with World's First Global 5G Modem. [Online]. Available: https://newsroom.intel.com/editorials/intel-accelerates-the-future-with-first-global-5g-modem/

[9] ITU, "Final Acts WRC-15, World Radiocommunication Conference," Tech. Rep., 2016.

[10] H. Tan, W. Li *et al.*, "The analysis on the candidate frequency bands of future mobile communication systems," *China Communications*, vol. 12, no. Supplement, pp. 140–149, 2015.

[11] M. Kassem *et al.*, "Future wireless spectrum below 6 GHz: A UK perspective," in *Proc. of IEEE DySPAN*, 2015.

[12] Ofcom, "3.8 GHz to 4.2 GHz band: Opportunities for Innovation," Ofcom, Call for Input, Apr. 2016.

[13] FCC, "ET Docket 10-174: Second Memorandum Opinion and Order in the Matter of Unlicensed Operation in the TV Broadcast Bands," FCC, Active Regulation, Sep. 2012.

[14] Z. Qin, Y. Gao *et al.*, "Wideband spectrum sensing on real-time signals at sub-nyquist sampling rates in single and cooperative multiple nodes," *IEEE Trans. on Signal Proc.*, vol. 64, no. 12, pp. 3106–3117, June 2016.

[15] Z. Qin, Y. Gao, and C. G. Parini, "Data-assisted low complexity compressive spectrum sensing on real-time signals under sub-nyquist rate," *IEEE Trans. on Wireless Communications*, vol. 15, no. 2, pp. 1174–1185, Feb 2016.

[16] FCC, "GN Docket 12-354: Amendment of the Commission's Rules with Regard to Commercial Operations in the 3550-3650 MHz Band," FCC, Order on Reconsideration, May 2016.

[17] Y. Hou, M. Li *et al.*, "Cooperative interference mitigation for heterogeneous multi-hop wireless networks coexistence," *IEEE Trans. on Wireless Communications*, vol. 15, no. 8, pp. 5328–5340, Aug. 2016.

[18] C. Ghosh, S. Roy, and D. Cavalcanti, "Coexistence challenges for heterogeneous cognitive wireless networks in TV white spaces," *IEEE Wireless Communications*, vol. 18, no. 4, pp. 22–31, Aug. 2011.

[19] A. Reina, G. Valentini *et al.*, "A design pattern for decentralised decision making," *PLoS ONE*, 2015.

[20] A. Reina, R. Miletitch *et al.*, "A quantitative micro-macro link for collective decisions: the shortest path discovery/selection example," *Swarm Intelligence*, vol. 9, pp. 75–102, 2015.

[21] Z. Guan and T. Melodia, "CU-LTE: Spectrally-efficient and fair coexistence between LTE and Wi-Fi in unlicensed bands," in *Proc. of IEEE INFOCOM*, Apr. 2016, pp. 1–9.

[22] Y. Li, F. Baccelli *et al.*, "Modeling and Analyzing the Coexistence of Wi-Fi and LTE in Unlicensed Spectrum," *IEEE Trans. on Wireless Communications*, vol. 15, no. 9, pp. 6310–6326, Sep. 2016.

[23] R. Ma, H. H. Chen, and W. Meng, "Dynamic Spectrum Sharing for the Coexistence of Smart Utility Networks and WLANs in Smart Grid Communications," *IEEE Network*, vol. 31, no. 1, pp. 88–96, Jan. 2017.

[24] H. Zhang, X. Chu *et al.*, "Coexistence of Wi-Fi and heterogeneous small cell networks sharing unlicensed spectrum," *IEEE Communications Magazine*, vol. 53, no. 3, pp. 158–164, Mar. 2015.

[25] E. Aryafar, *et al.*, "RAT selection games in HetNets," in *Proc. of IEEE INFOCOM*, April 2013, pp. 998–1006.

[26] F. M. Abinader, E. P. L. Almeida *et al.*, "Enabling the coexistence of LTE and Wi-Fi in unlicensed bands," *IEEE Communications Magazine*, vol. 52, no. 11, pp. 54–61, Nov. 2014.

[27] Q. Chen, G. Yu *et al.*, "Cellular Meets WiFi: Traffic Offloading or Resource Sharing?" *IEEE Trans. on Wireless Communications*, vol. 15, no. 5, pp. 3354–3367, May 2016.

[28] Y. Song, K. W. Sung, and Y. Han, "Coexistence of Wi-Fi and Cellular With Listen-Before-Talk in Unlicensed Spectrum," *IEEE Communications Letters*, vol. 20, no. 1, pp. 161–164, Jan. 2016.

[29] M. Hirzallah, W. Afifi, and M. Krunz, "Full-Duplex-Based Rate/Mode Adaptation Strategies for Wi-Fi/LTE-U Coexistence: A POMDP Approach," *IEEE Journal on Selected Areas in Communications*, vol. 35, no. 1, pp. 20–29, Jan. 2017.

[30] B. Chen, J. Chen *et al.*, "Coexistence of LTE-LAA and Wi-Fi on 5 GHz With Corresponding Deployment Scenarios: A Survey," *IEEE Communications Surveys Tutorials*, vol. 19, no. 1, pp. 7–32, 1Q 2017.

[31] X. Yuan *et al.*, "Coexistence between Wi-Fi and LTE on Unlicensed Spectrum: A Human-Centric Approach," *IEEE Journal on Selected Areas in Communications*, vol. 35, no. 4, pp. 964–977, April 2017.

[32] M. A. Raza, S. Park, and H. N. Lee, "Evolutionary Channel Sharing Algorithm for Heterogeneous Unlicensed Networks," *IEEE Trans. on Wireless Communications*, vol. 16, no. 7, pp. 4378–4389, July 2017.

[33] D. Zhang, Q. Liu *et al.*, "Ecology-Based Coexistence Mechanism in Heterogeneous Cognitive Radio Networks," in *Proc. of IEEE GLOBECOM*, Dec. 2015, pp. 1–6.

[34] A. S. Cacciapuoti, M. Caleffi, and L. Paura, "Optimal Strategy Design for Enabling the Coexistence of Heterogeneous Networks in TV White Space," *IEEE Trans. on Vehicular Technology*, vol. 65, no. 9, pp. 7361–7373, Sep. 2016.

[35] R. Mazumdar, L. G. Mason, and C. Douligeris, "Fairness in Network

Optimal Flow Control: Optimality of Product Forms," *IEEE Trans. on Communications*, vol. 39, no. 5, May 1991.
[36] Ofcom, "Regulatory requirements for white space devices in the UHF TV band," Ofcom, Active Regulation, July 2012.
[37] T. D. Seeley, P. K. Visscher *et al.*, "Stop Signals Provide Cross Inhibition in Collective Decision-Making by Honeybee Swarms," *Science*, vol. 335, no. 6064, pp. 108–111, 2012.
[38] D. Pais *et al.*, "A Mechanism for Value-Sensitive Decision-Making," *PLoS ONE*, vol. 8, no. 9, pp. 1–9, Sept. 2013.
[39] A. Reina, J. A. R. Marshall, V. Trianni, and T. Bose, "Model of the best-of-N nest-site selection process in honeybees," *Physical Review E*, vol. 95, no. 5, pp. 052 411–15, 2017.
[40] T. C. Aysal, M. E. Yildiz, A. D. Sarwate, and A. Scaglione, "Broadcast Gossip Algorithms for Consensus," *IEEE Trans. on Signal Processing*, vol. 57, no. 7, pp. 2748–2761, July 2009.
[41] Y. C. Liang, Y. Zeng, E. C. Y. Peh, and A. T. Hoang, "Sensing-Throughput Tradeoff for Cognitive Radio Networks," *IEEE Trans. on Wireless Communications*, vol. 7, no. 4, pp. 1326–1337, Apr. 2008.
[42] P. Moretti, S. Y. Liu, A. Baronchelli, and R. Pastor-Satorras, "Heterogenous mean-field analysis of a generalized voter-like model on networks," *The European Physical Journal B*, vol. 85, no. 3, pp. 1–6, 2012.
[43] H. Silk, M. Homer, and T. Gross, "Design of Self-Organizing Networks: Creating Specified Degree Distributions," *IEEE Trans. on Network Science and Engineering*, vol. 3, no. 3, pp. 147–158, 2016.
[44] A. Reina *et al.*, "Psychophysical laws and the superorganism," *Scientific Reports*, vol. 8, no. 1, p. 4387, 2018.
[45] K. Harrison and A. Sahai, "Allowing sensing as a supplement: An approach to the weakly-localized whitespace device problem," in *Proc. of IEEE DYSPAN*, April 2014, pp. 113–124.

Marcello Caleffi (M'12, SM'16) received the M.S. degree (summa cum laude) in computer science engineering from the University of Lecce, Lecce, Italy, in 2005, and the Ph.D. degree in electronic and telecommunications engineering from the University of Naples Federico II, Naples, Italy, in 2009. Currently, he is with the DIETI Department, University of Naples Federico II, and with the National Laboratory of Multimedia Communications, National Inter-University Consortium for Telecommunications (CNIT). From 2010 to 2011, he was with the Broadband Wireless Networking Laboratory at Georgia Institute of Technology, Atlanta, as visiting researcher. In 2011, he was also with the NaNoNetworking Center in Catalunya (N3Cat) at the Universitat Politecnica de Catalunya (UPC), Barcelona, as visiting researcher. Since July 2018, he held the Italian national habilitation as *Full Professor* in Telecommunications Engineering. His work appeared in several premier IEEE Transactions and Journals, and he received multiple awards, including *best strategy* award, *most downloaded article* awards and *most cited article* awards. Currently, he serves as editor for IEEE Communications Letters and Elsevier Ad Hoc Networks; moreover, he serves as associate technical editor for IEEE Communications Magazine and IEEE Access. He has served as Chair, TPC Chair, Session Chair, and TPC Member for several premier IEEE conferences. In 2016, he was elevated to IEEE Senior Member and in 2017 he has been appointed as Distinguished Lecturer from the IEEE Computer Society.

Vito Trianni is a permanent researcher at the Institute of Cognitive Sciences and Technologies of the Italian National Research Council (ISTC-CNR). He received the Ph.D. in Applied Sciences at the Universit Libre de Bruxelles (Belgium) in 2006, a master in Information and Communication Technology from CEFRIEL (Italy) in 2001, and the M.Sc. in Computer Science Engineering at the Politecnico di Milano (Italy) in 2000. He has authored about 100 publications, among which 1 book and 32 publications in international journals with peer review. Vito Trianni's research mainly involves swarm intelligence and swarm robotics studies, with particular emphasis on the design and analysis of complex self-organizing systems and distributed cognitive processes. He pioneered the domain of Evolutionary Swarm Robotics, that is, the synthesis of collective behaviors for robotic swarms through the exploitation of evolutionary robotics techniques. More recently, he is also conducting research on the analysis and design of large-scale decentralised systems, not limited to swarm robotics systems (e.g., cognitive radio networks, cyber-physical and socio-technical systems).

Angela Sara Cacciapuoti (M'10, SM'16) received the Ph.D. degree in Electronic and Telecommunications Engineering in 2009, and the 'Laurea summa cum laude in Telecommunications Engineering in 2005, both from the University of Naples Federico II. Since April 2017, she held the Italian Habilitation as "Associate Professor" in Telecommunications Engineering and since July 2018, she held the Italian Habilitation as "Full Professor" in Telecommunications Engineering. Currently, she is a Tenure-Track Assistant Professor at the Department of Electrical Engineering and Information Technology, University of Naples Federico II. Prior to that, she was a visiting researcher at the Georgia Institute of Technology (USA) and at the NaNoNetworking Center in Catalunya (N3Cat), School of Electrical Engineering, Universitat Politecnica de Catalunya (Spain). Her work appeared in the first tier IEEE journals and she received different awards including the elevation to the grade of IEEE Senior Member in February 2016, most downloaded article and most cited article awards, and outstanding young faculty/researcher fellowships for conducting research abroad. Angela Sara serves as Editor/Associate Editor for the journals: IEEE Trans. on Communications, IEEE Communications Letters, Computer Networks (Elsevier) Journal and IEEE Access. She was awarded with the 2017 Exemplary Editor Award of IEEE Communications Letters. Since 2016, she is a board member of the IEEE ComSoc Young Professionals (YPs) Standing Committee and, since 2018 of the IEEE ComSoc Women in Communications Engineering (WICE) Standing Committee. In February 2017, she has been appointed Award Co-Chair of the N2Women Board and in July 2017, she has been elected Treasurer of the IEEE Women in Engineering (WIE) Affinity Group (AG) of the IEEE Italy Section.